

# SERS and EQCM studies on the effect of allyl thiourea on copper dissolution and deposition in aqueous sulfuric acid

Guo-Liang Chen · Heng Lin · Jiang-Hong Lu · Li Wen ·  
Jian-Zhang Zhou · Zhong-Hua Lin

Received: 4 October 2007 / Accepted: 13 May 2008 / Published online: 3 June 2008  
© Springer Science+Business Media B.V. 2008

**Abstract** We investigated the effect of allyl thiourea (ATU) on both the electrodeposition and electrodisolution of copper in aqueous sulfuric acid by combining cyclic voltammetry (CV) with electrochemical quartz crystal microbalance (EQCM) studies and surface enhanced Raman spectroscopy (SERS). The results demonstrated that the two-electron transfer reaction is the predominant process for the copper dissolution–deposition process in 1.0 M H<sub>2</sub>SO<sub>4</sub> solution not containing ATU in the potential range  $-0.65$  to  $0.05$  V versus SCE. In comparison, the copper dissolution–deposition process in 1.0 M H<sub>2</sub>SO<sub>4</sub> solution containing ATU corresponds to a one-electron transfer reaction. The spectral features observed from the SERS studies showed at molecular level that ATU can be adsorbed tilted to the copper electrode surface and that coordination occurs via the sulfur atom. The secondary amino group is nearer to the surface than the primary amino group. SO<sub>4</sub><sup>2-</sup> and HSO<sub>4</sub><sup>-</sup> can be coadsorbed on the protonated  $-\text{NH}(\text{CH}_2\text{CHCH}_2)$  groups.

**Keywords** Allyl thiourea · Copper · EQCM · SERS

## 1 Introduction

Thiourea (TU) is widely used as a brightener during copper deposition [1–8]. It functions by interacting strongly with the electrode surface and altering the mode of deposition to produce coatings that are microscopically smooth and thus appear bright. TU is also used as an acid inhibitor in industrial operations, such as pickling, descaling, cleaning, and acidisation of oil wells, to protect metals and alloys [9–11]. Consequently, the effect of TU on both the electrodeposition and electrodisolution of copper from acidic sulfate electrolytes has been studied in detail with a variety of techniques [12–22]. In the presence of TU, the electrodeposition and electrodisolution of copper become relatively complex due to the concurrence of electrochemical reactions at the copper/TU-containing solution interface [23, 24], the chemical reactions between TU and copper ions in the solution [25], and the strong chemisorption of TU and its reaction products [26].

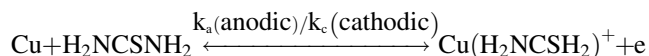
The interaction of TU with a copper electrode in aqueous sulfuric acid has been examined by several researchers using the SERS technique [17–22]. Such studies have yielded important information on the direct interaction of TU with the electrode surface in situ. There is general agreement that TU is strongly chemisorbed and that the process of TU adsorption depends on the applied potential, the bulk concentration of TU, and the kind of the supporting electrolyte [13]. The TU molecule is adsorbed on the copper surface via the sulfur atom. In relation to this, Loo reported the vibrational frequency for the Cu–S stretching mode to be at  $288\text{ cm}^{-1}$  [17]. Furthermore, it is evident that the adsorption of TU at the copper electrode is accompanied by the co-adsorption of sulfate ions.

Alodan et al. examined the effect of TU on copper dissolution and deposition in sulfuric acid solutions using

G.-L. Chen (✉) · L. Wen · J.-Z. Zhou · Z.-H. Lin  
Department of Chemistry, State Key Laboratory for Physical  
Chemistry of Solid Surfaces, College of Chemistry and  
Chemical Engineering, Xiamen University,  
Xiamen 361005, China  
e-mail: chengl259@263.net

G.-L. Chen · H. Lin · J.-H. Lu  
Department of Chemistry, Zhangzhou Normal University,  
Zhangzhou 363000, China

the EQCM technique [15]. It was shown that TU forms complexes with cuprous ions in the solution, which shift the open circuit potential of the copper electrode in a negative direction and cause copper to dissolve to cuprous species even in sulfate media. At more positive potentials, TU reacts with cupric ions and forms a complex, while at a sufficient concentration of the cupric-TU complex, a sulfate complex film forms. The QCM results suggest that the copper electrode dissolves to the cuprous state in the presence of TU in sulfate media according to the following reaction:



In recent years, N-substituted thioureas have also been considered as possible additives for copper electrodeposition [27, 28] and as inhibitors for iron corrosion [29]. Allyl thiourea (ATU,  $\text{CH}_2=\text{CHCH}_2\text{NHCNSH}_2$ ) is an important derivative of TU. ATU has been found to have a better inhibiting effect than TU and other derivatives, such as ethylene thiourea and phenylthiourea, for transition metals [30]. As compared to TU and other derivatives, ATU has a more asymmetric structure. The molecule of ATU contains methylene connected with ethylene and a N atom, and it cannot cause a conjugative effect between C=C and C=S. Therefore, the negative charge density around the sulfur atom is still quite high. At the same time, ATU may undergo hyperconjugation between methylene and C=C, and may greatly increase the degree of freedom of the C=C space circumrotation. This means that the ATU molecule may act as a bidentate ligand that donates electron via the sulfur atom and  $\pi$ -bond [30].

Recently, we have advanced copper electroless plating technology by chemical displacement on an iron surface from acidic cupric sulfate solutions containing a small quantity of ATU, which is suitable for producing  $\text{CO}_2$  gas-shielded welding wire. As compared to TU, ATU can greatly increase adhesion and ameliorate the colour and lustre of the deposit. It is important to obtain information about the interaction of ATU and copper for a better understanding of the particular effect of ATU on copper inhibition and electrodeposition. To the best of our knowledge, no other paper describes the effect of ATU on copper dissolution and deposition at a molecular level and in a quantitative manner.

In this work, we studied the effect of ATU on copper dissolution and deposition in sulfuric acid solutions by combining CV, EQCM, and SERS. We showed that ATU may adsorb on the copper surface, inhibit copper electrode processes, and change the mechanism of the anodic dissolution and cathodic deposition of copper. The results give some insights into these processes.

## 2 Experimental details

Current and frequency changes were measured simultaneously as a function of the applied potential by an EQCM (Seiko EG&G Parc Instruments), which was equipped with a model 263 potentiostat/galvanostat and a QCA-917.

In the EQCM experiments, the working electrode was one side of an AT-cut quartz crystal with the fundamental frequency  $f_0 = 9$  MHz covered on both sides with a platinum film (the electrode area was  $0.196 \text{ cm}^2$ ). The platinum surface was cleaned by rinsing with Millipore water followed by potential cycling between  $-0.25$  and  $1.4$  V in  $0.1 \text{ M H}_2\text{SO}_4$  solution, until stable  $j$ - $E$  curve and  $(\Delta f) - E$  variation were recorded. Copper was plated on top of the platinum film from  $0.1 \text{ M}$  cupric sulfate and  $1 \text{ M}$  sulfuric acid solution at  $-10 \text{ mA cm}^{-2}$  until a thickness of about  $2 \mu\text{m}$  was reached (denoted as Pt/Cu thereafter). The reference electrode was a KCl-saturated calomel electrode (SCE), separated from the cell by a bridge made of a stopcock of two ends containing the solution. The counter electrode was a platinum foil with a geometric area of  $1 \text{ cm}^2$ . All the potential values given below refer to the SCE. The sweep rate was  $5 \text{ mV s}^{-1}$ . Electrochemical measurements were made in a glass compartment with  $30 \text{ mL}$  capacity. The cell had a special Teflon cover with holes designed to host the auxiliary and working electrodes and the degassing tubes. The Luggin compartment was connected directly to the cell body.

The relationship between surface mass change and resonant frequency change for an EQCM electrode is given by the Sauerbrey Equation [31]:

$$\Delta f = f - f_0 = -2\Delta m f_0^2/A(\mu\rho)^{1/2} = -C_f\Delta m, \quad (1)$$

where  $f_0$  is the fundamental frequency of the crystal in Hz,  $\Delta f$  is the frequency change in Hz,  $\Delta m$  is the surface mass change per unit area ( $\text{g cm}^{-2}$ ),  $A$  is the area of the electrode,  $\mu$  is the shear modulus ( $\mu = 2.947 \times 10^{11} \text{ g cm}^{-1} \text{ s}^{-2}$ ),  $\rho$  is the density ( $\rho = 2.648 \text{ g cm}^{-3}$ ) of quartz, and  $C_f$  is the sensitivity factor of the quartz crystal in  $\text{Hz } \mu\text{g}^{-1}$ .

The sensitivity factor for the EQCM used in the studies was determined using the potentiostatic electrodeposition of copper ( $1 \text{ M H}_2\text{SO}_4 + 0.1 \text{ M CuSO}_4$ ), in which the charge densities were used to calculate the mass values, and the resonant frequencies were measured experimentally. The value of the sensitivity factor thus obtained was  $902 \text{ Hz } \mu\text{g}^{-1}$  assuming 100% current efficiency [6], which is smaller than the calculated value of  $915 \text{ Hz } \mu\text{g}^{-1}$ , using Sauerbrey's equation. The difference observed between the experimental sensitivity coefficient and its theoretical value is attributed to the difference between the resonant frequency with the crystal oscillating in the vacuum and in the solution [32].

Raman spectra were recorded on a confocal microprobe Raman system (LabRam 1) using an aircooled He–Ne Laser operating at 632.8 nm. The working electrode used for the spectroelectrochemical measurements was machined from commercially available 99.99% pure copper with a 6 mm diameter exposed surface. Prior to all experiments, the electrode surface was abraded with 1,200 grade wet and dry silicon carbide paper and was thoroughly rinsed with purified water. The usual electrochemical pretreatment for the activation of copper electrodes consisted of 2–3 oxidation-reduction square pulses, which stepped the applied potential from 0.4 V (5 s) to  $-0.4$  V (15 s) in 0.1 M KCl solution, and the initial and final potentials were  $-0.4$  V. The pretreatment and roughening procedure and additional details have been given elsewhere [33]. For the collection of potential-dependent SERS spectra, the electrode potential was stepped from  $-0.65$  V to 0.0 V at an interval of 0.10 V, and then stepped back to  $-0.65$  V.

All the chemicals were of analytical grade, and the solutions were prepared using Milli-Q water (Millipore Ltd, Japan). All experiments were carried out in solutions deaerated with purified nitrogen and at room temperature ( $\sim 22$  °C).

### 3 Results and discussion

#### 3.1 CV and EQCM Studies

##### 3.1.1 Cathodic deposition and anodic dissolution of copper in aqueous sulfuric acid

Figure 1 shows the cyclic voltammogram (Fig. 1a) and the associated frequency change (Fig. 1b) in 1.0 M  $\text{H}_2\text{SO}_4$  solution, measured on a Pt/Cu surface in the potential region between  $-0.60$  and 0.05 V. The anodic dissolution of copper begins at about  $-0.05$  V (Fig. 1a). The frequency starts to increase at about the same potential. The cathodic

deposition of the copper ions formed in the preceding potential scan begins at about 0.00 V (Fig. 1a) and ends at about  $-0.30$  V during the reverse scan; this is accompanied by a simultaneous frequency decrease (mass increase). The frequency plot does not return to its initial value after the scan, indicating that the mass decrease due to cupric ion dissolution was larger than the mass increase due to cupric ion deposition after the scan. That is to say, some of the  $\text{Cu}^{2+}$  produced during oxidation will be dispersed into the bulk of the solution and thus be unavailable for deposition during the reverse scan. Finally, starting from  $-0.36$  V at the reverse scan, the cathodic current increases steadily due to the contribution of hydrogen evolution reaction on copper.

For characterising the electrochemical and other processes at the electrode surface, the primary EQCM data are usually treated in different ways. An often straightforward option [34–36] is to form an  $\Delta f$  versus  $\Delta Q$  curve and use the Sauerbrey equation and Faraday's law to calculate a parameter  $M/n$  from the slope of such a curve:

$$M/n = (-d\Delta f/d\Delta Q) F/C_f \quad (2)$$

where  $M$  is the molar mass of the species responsible for the mass change,  $n$  is the number of electrons involved in the charge transfer process,  $F$  is the Faraday constant ( $96,500 \text{ C mol}^{-1}$ ), and  $\Delta Q$  is the experimentally measured charge changes. By using the value of  $M/n$ , the molar mass of the deposited or dissolved species on the electrode surfaces can be ascertained to provide a quantitative basis for further judging the electrochemical mechanisms of electrode reactions. It should be emphasized that the experimental  $M/n$  values obtained using this method do not involve any hypothesis about the reaction mechanisms but are directly based on the primary data. Their main benefit is that the corresponding theoretical values are easily calculated for suggested reactions. The theoretical  $M/n$  is simply the molar mass of the deposit divided by the number of electrons involved in the reaction [16].

**Fig. 1** Cyclic Voltammogram (a) and frequency response (b) for Pt/Cu electrode in 1.0 M  $\text{H}_2\text{SO}_4$  solution, Sweep rate 5 mV/s

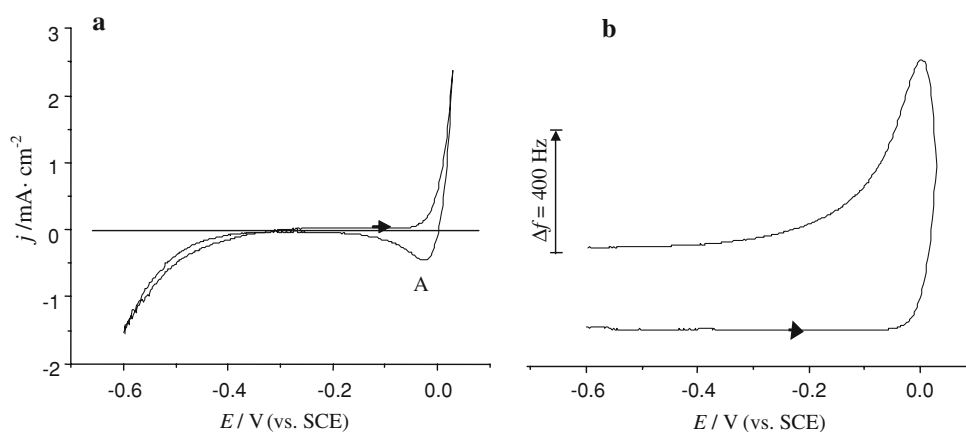


**Fig. 2** Plot of  $\Delta f$  versus  $\Delta Q$  of Pt/Cu electrode in 1.0 M  $\text{H}_2\text{SO}_4$  solution for anodic reaction (a) and cathodic reaction (b)

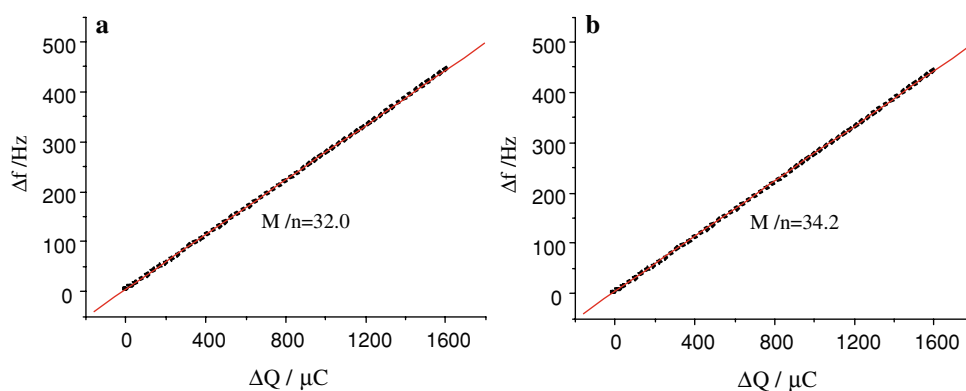


**Fig. 3** Cyclic Voltammogram (a) and frequency response (b) for Pt/Cu electrode in 1.0 M  $\text{H}_2\text{SO}_4$  + 11 mM ATU, Sweep rate  $5 \text{ mV s}^{-1}$

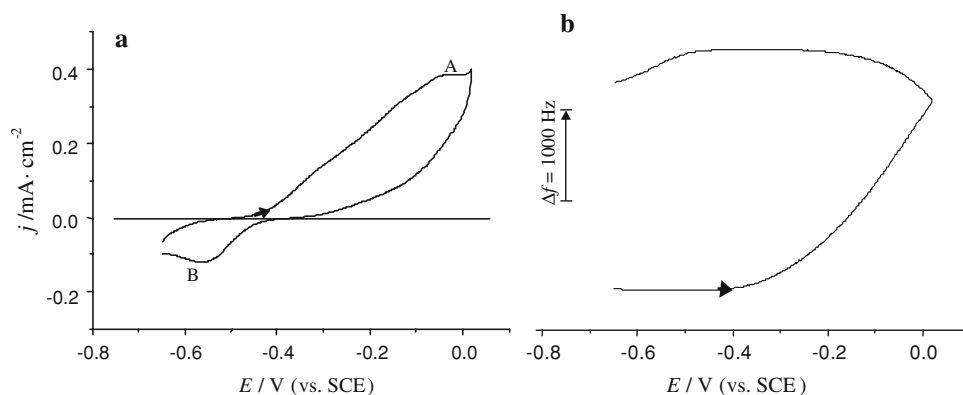


Figure 2 shows the  $\Delta f$  versus  $\Delta Q$  plot obtained from the data in Fig. 1, which is for the anodic reaction (Fig. 2a) and for the cathodic reaction (Fig. 2b), respectively. An  $M/n$  value of  $32.0 \text{ g mol}^{-1}$  is obtained in the potential range from  $-0.05 \text{ V}$  at the forward scan to  $0.00 \text{ V}$  at the reverse scan. This value corresponds to the two-electron oxidation of copper (Eq. 3):



Theoretically  $M/n = 63.54/2 = 31.77 \text{ g mol}^{-1}$ . The cathodic deposition of copper yields an  $M/n$  value of  $34.2 \text{ g mol}^{-1}$  between  $0.00$  and  $-0.30 \text{ V}$  during the reverse scan, which corresponds to the reverse of Eq. 3.

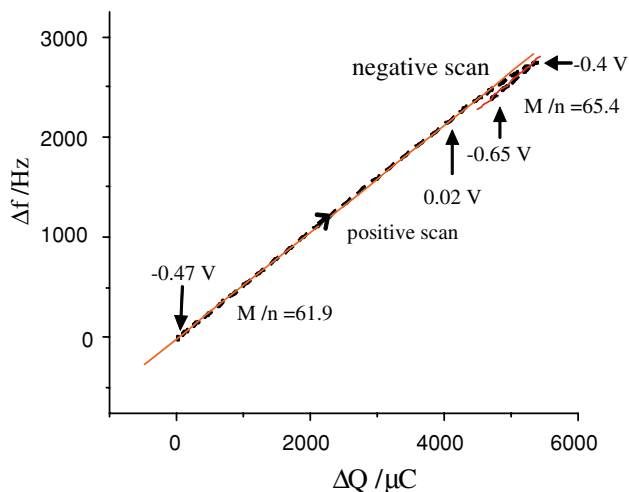
### 3.1.2 Cathodic deposition and anodic dissolution of copper in a sulfuric acid solution containing ATU

Figure 3 shows the cyclic voltammogram (Fig. 3a) and the associated frequency change (Fig. 3b) in a solution containing 11 mM ATU and 1.0 M  $\text{H}_2\text{SO}_4$ , measured on a Pt/Cu surface. The anodic current begins to flow at about  $-0.40 \text{ V}$ , which is much more negative than that when the scans are measured in the solution without ATU. In the successive potential scan, the anodic current increases, and a main current plateau A near  $-0.06 \text{ V}$  is observed. Only

one reduction peak B appears at about  $-0.53 \text{ V}$  at the reverse scan. As compared to Fig. 1a (without ATU), the current in Fig. 3a (with ATU) is much lower, indicating that ATU may inhibit copper electrode processes.

The frequency increases (mass decreases) in the potential range from  $-0.40 \text{ V}$  at the forward scan to  $-0.40 \text{ V}$  at the reverse scan. In the potential range between  $-0.40$  and  $-0.65 \text{ V}$  where the cathodic current peak B was observed, the frequency starts to decrease slowly. Also the frequency does not return to its initial value by the end of the scan.

Figure 4 shows the frequency change in Fig. 3b as a function of the charge consumed. An  $M/n$  value of  $61.9 \text{ g mol}^{-1}$  in a sulfuric acid solution containing ATU is obtained from  $-0.40 \text{ V}$  at the forward scan to  $-0.40 \text{ V}$  at the reverse scan. This is most probably due to the one-electron oxidation of copper. The cathodic deposition of copper yields an  $M/n$  value of  $65.4 \text{ g mol}^{-1}$  between  $-0.40$  and  $-0.65 \text{ V}$  at the reverse scan, which corresponds to the one-electron reduction of copper. These results are similar to those of TU [15]. This larger  $M/n$  value may be due to morphology changes on the electrode surface as observed earlier [34] with Cu–Se compounds. Roughening of the deposit is known to cause liquid trapping in surface cavities, which thereby increases the mass of the deposit [37]. Obviously, the  $M/n$  values for copper dissolution–



**Fig. 4** Plot of  $\Delta f$  versus  $\Delta Q$  of Pt/Cu electrode in 11 mM ATU + 1.0 M  $H_2SO_4$ , arrows indicate the potential corresponding to one in the CV plot (Fig. 3a)

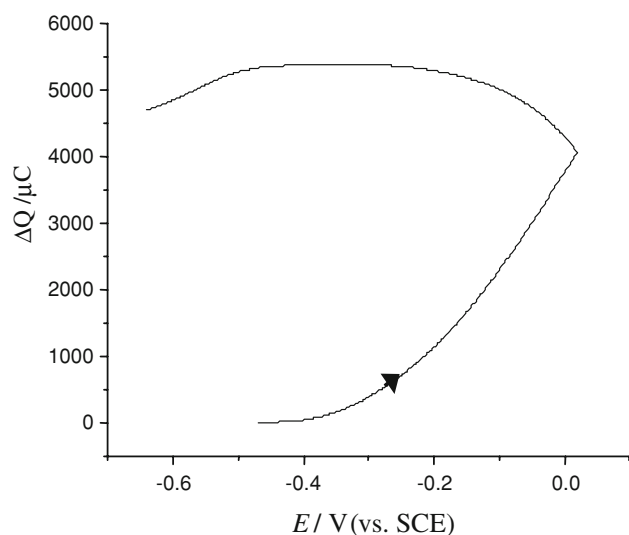


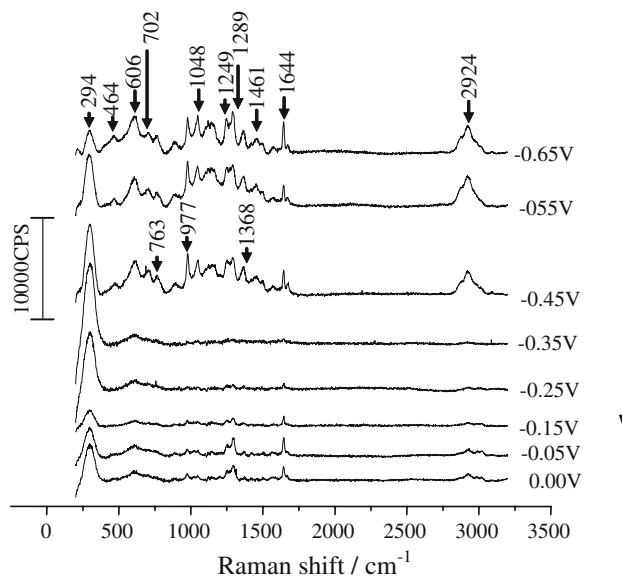
**Fig. 5** Plot of  $\Delta Q$  versus  $E$  of Pt/Cu electrode in 11 mM ATU + 1.0 M  $H_2SO_4$

deposition processes measured in the presence of ATU are different from those obtained in the absence of ATU, indicating that ATU may change the mechanism of the anodic dissolution and cathodic deposition of copper and produce Cu (I) species.

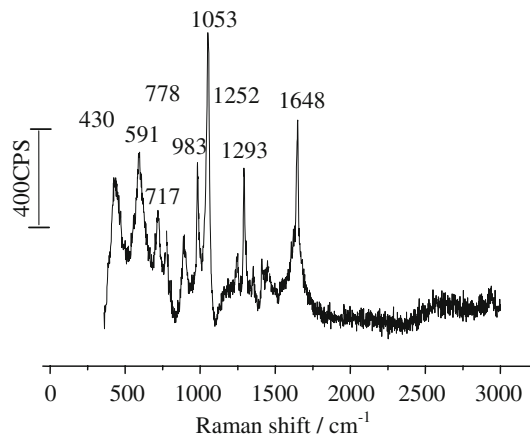
Figure 5 shows the charge that passes through the electrode during the potential scan. The shape of the charge plot is similar to that of the frequency plot. Furthermore, the final value of the charge remains above zero after the potential scan.

### 3.2 In situ SERS studies

Typical in situ SERS spectra of an electrochemically roughened copper electrode in a 1.0 M  $H_2SO_4$  + 11 mM



**Fig. 6** SERS spectra of adsorbed ATU on a roughened Cu electrode in 11 mM ATU + 1.0 M  $H_2SO_4$  at different potentials from  $-0.65$  V to  $0.00$  V

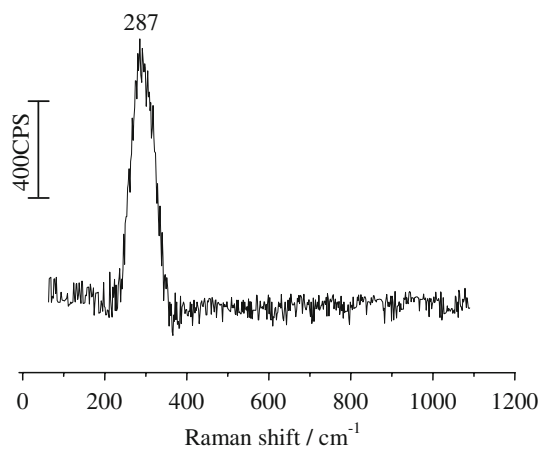


**Fig. 7** Normal Raman spectrum of 0.5 M ATU + 1.0 M  $H_2SO_4$  solution

ATU solution with change of the electrode potential from  $-0.65$  to  $0.00$  V are given in Fig. 6. Below  $-0.65$  V, the spectral intensity is affected by hydrogen evolution. The normal Raman spectrum of a 0.5 M ATU+1.0 M  $H_2SO_4$  solution is also given in Fig. 7 to facilitate comparison and discussion on the interaction of ATU with a copper electrode in a sulfuric acid solution. Assignment of the different vibrational bands is performed by combining the information from the spectra and from the literature [17–22]. A summary of SERS vibrational frequencies and their detailed assignments is given in Table 1. These spectra have the following features.

**Table 1** Frequencies and assignment of vibrational bands in the normal Raman spectrum and SERS spectra of ATU

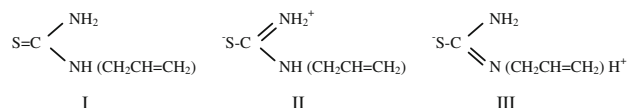
Raman frequencies of 1.0 M H <sub>2</sub> SO <sub>4</sub> + 0.5 M ATU solution/cm <sup>-1</sup>	SERS frequencies of ATU at Cu electrode/cm <sup>-1</sup>	Assignment
	294	Cu–S stretching
430	464	NCN bending
591	606	SCNN out-of plane bending
717	702	C=S stretching
778	762	C=S stretching
983	977	SO <sub>4</sub> <sup>2-</sup> stretching
1,053	1,048	HSO <sub>4</sub> <sup>-</sup> stretching
1,252	1,249	C–H in plane deformation
1,293	1,289	C–H in plane deformation
	1,368	Combined C–S/C–N stretching
	1,461	NCN asymmetric stretching
1,648	1,644	C=C stretching
	2,924	C–H stretching

**Fig. 8** SERS spectrum obtained on a roughened copper electrode after being immersed in 0.1 M Na<sub>2</sub>S solution at the open circuit potential

(a) Obviously, the most intense band appears at around 294 cm<sup>-1</sup> in the SERS spectra. Considering the molecular structure of ATU, we assume that the 294 cm<sup>-1</sup> band may arise from the Cu–S stretching vibration. To verify this, the copper electrode was directly immersed in 0.1 M Na<sub>2</sub>S solution, and a Raman spectrum (Fig. 8) was acquired at the open circuit potential, which shows the same band as that in Fig. 6 at around 287 cm<sup>-1</sup>. Hence, the SERS spectra presented in Fig. 6 strongly support the claim that ATU

adsorbs at the copper surface, and that coordination occurs via the sulfur atom. This behaviour is similar to the findings of Loo that thiourea adsorbs at the copper surface and that coordination occurs via the sulfur atom [17]. When the potential is changed from -0.65 to -0.45 V, where copper is not electro-dissolved (see Fig. 3), the relative intensity of the bands at 287 cm<sup>-1</sup> increases, which is a result of the increased adsorption of ATU at the electrode surface. Accordingly, adsorption of ATU at the copper electrode is dependent on the electrode potential.

(b) The SERS spectra in Fig. 6 exhibit new bands and frequency shifts of vibrational modes in relation to the ATU solution spectrum. The C=S stretching (702 and 762 cm<sup>-1</sup>) and the NCN bending (464 cm<sup>-1</sup>) modes have the largest frequency shift compared with their solution values (717, 778 and 430 cm<sup>-1</sup>, respectively). The new signals at 1,368 and 1,461 cm<sup>-1</sup> in the ATU surface spectra correspond to the vibrational modes of combined C–S/C–N stretching [18] and NCN asymmetric stretching [38], respectively, which are greatly enhanced after adsorption. These results indicate short-range interactions between the copper surface and ATU. TU presents three canonical forms [39]. Similarly, we assume that ATU may present the following canonical forms I, II, and III:



If ATU is bonded to the copper surface through a sulfur atom, the contributions from the canonical forms II and III will increase, decreasing the double bond character of the C–S to that for a single bond and increasing the C–N to that for a double bond. In this way, the frequency of the C=S stretching mode should be lower than 717 or 778 cm<sup>-1</sup>, and the frequency of the NCN stretching mode should be higher than 430 cm<sup>-1</sup> (values of 717, 778, and 430 cm<sup>-1</sup> corresponding to the ATU solution spectrum). All these facts further support the possibility that ATU adsorbs on the copper surface through its sulfur atom and that the molecular structure of ATU changes significantly after adsorption.

(c) An analysis of the relative intensity change of the bands at 606 cm<sup>-1</sup> with potential may provide some orientation information on the adsorption of ATU. According to the surface selection rule of SERS, those vibrational modes with polarisability perpendicular to the surface can be greatly enhanced, whereas those with polarisability parallel to the surface will not be enhanced [33]. The 606 cm<sup>-1</sup> band, designated as SCNN out of the plane bending mode, increases in intensity with increasing negative potential. The enhancement of this mode with

increasing negative potential indicates that this vibrational mode may have a polarisability perpendicular to the surface. According to its molecular structure, if this type of vibration has a polarisability perpendicular to the surface, the ATU molecular orientation has to be flat on or tilt to the surface at a more negative potential.

(d) A few bands near 1249, 1289, 1644, and 2924  $\text{cm}^{-1}$  may be seen on the SERS spectra, which are attributable to the C–H in-plane deformation, C=C stretching, and C–H stretching vibrational modes, respectively [22]. The intensity of these bands may change with electrode potential, but no observable changes in band position are noted. These results indicate that the C=C bond in the  $\text{CH}_3\text{CH}=\text{CH}$ - group is not directly attached to the copper surface and that the secondary amino group is nearer the surface than the primary amino group. Another point that supports this conclusion is the observation that the bands at 1249, 1289 and 1644  $\text{cm}^{-1}$  are only slightly changed from the corresponding bands in the solution spectra. Thus, the whole ATU molecule tends to adsorb in a tilted way through its  $\text{CH}_3\text{CH}=\text{CH}$ - group towards the copper electrode surface.

(e) It has been reported that the frequencies of aqueous  $\text{SO}_4^{2-}$  and  $\text{HSO}_4^-$  were 997 and 1057  $\text{cm}^{-1}$  respectively, 971 and 1,052  $\text{cm}^{-1}$  for two species adsorbed on copper [18]. From Fig. 6, it is evident that the SERS spectra also show two strong bands at 977 and 1,048  $\text{cm}^{-1}$  arising from the stretching mode of  $\text{SO}_4^{2-}$  and  $\text{HSO}_4^-$  respectively, and the frequencies of these bands are not shifted with potential. This means that  $\text{SO}_4^{2-}$  and  $\text{HSO}_4^-$  are not directly adsorbed on the Cu surface, but rather co-adsorbed with ATU as their frequencies are different from those of free sulfate ions. Considering that the hyperconjugation of alkyl often increases the alkalinity of aliphatic amine, we can conclude that the  $-\text{NH}(\text{CH}_2\text{CHCH}_2)$  group in the ATU molecule may be protonated more easily than the  $-\text{NH}_2$  group. As the ATU molecule adsorbs at the copper surface via the sulfur atom (form III), we assume that  $\text{SO}_4^{2-}$  and  $\text{HSO}_4^-$  are quite likely to coadsorb on the protonated  $-\text{NH}(\text{CH}_2\text{CHCH}_2)$  groups.

(f) As shown above (Fig. 3), copper starts to be electro-dissolved at about  $-0.35$  V. The spectra in Fig. 6 show that the relative intensity of the 294  $\text{cm}^{-1}$  peak is probably at its highest value at  $-0.35$  V while the other peaks have disappeared. The 294  $\text{cm}^{-1}$  peak is still large at  $-0.25$  V. This peak seems to behave differently than the others, at least at these potentials. The appearance of the band at 294  $\text{cm}^{-1}$  in the whole potential range indicates that ATU is adsorbed on the Cu surface through the S atom. In the forward scan, its coverage increases as the potential shifts from  $-0.65$  to  $-0.35$  V. When the potential increases further, dissolution occurs, which may decrease the SERS activity and ATU coverage. As a result, the Cu–S band

exhibits a maximal SERS signal at about  $-0.35$  V. During Cu dissolution, the ATU is also dynamically adsorbed on the Cu surface, which may decrease the SERS enhancement of the group (e.g., C–H) not attached directly to the Cu surface. Therefore, their SERS signals can hardly be seen in the potential range  $-0.35$  to 0.00 V.

Figure 9 presents the SERS spectra of adsorbed ATU on a roughened copper electrode in a 1.0 M  $\text{H}_2\text{SO}_4$  + 11 mM ATU solution from 0.00 V to  $-0.65$  V immediately after completion of the scan shown in Fig. 6. Comparison of Figs. 6 and 9 shows some interesting differences. The spectra in Fig. 9 change much less with potential than do those in Fig. 6. The spectra in Fig. 9 from 0.00 to  $-0.35$  V correspond to conditions when metal dissolution, not deposition, is occurring (see Fig. 3). Most of the bands listed in Table 1 appear in the spectra. Yet, over the same potential range when the scan is proceeding in the forward direction (as shown in Fig. 6) when metal dissolution is also occurring, most bands have disappeared. Based on this, it appears that some ATU is adsorbing during dissolution when the electrode potential is decreasing from 0.0 to  $-0.35$  V during the reverse scan, but not during dissolution over the same potential range during the forward scan. Less dissolution occurs during the reverse scan than during the forward scan. This may be due to the amount of metal dissolution affecting the ability to detect adsorbed states so that the larger amount of dissolution during the forward scan is masking adsorption. At  $-0.35$  V, all the SERS signals are small, which may be attributed to lower SERS enhancement.

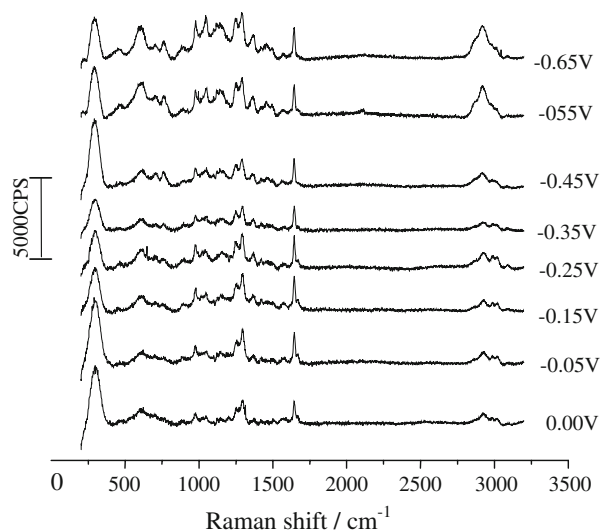


**Fig. 9** SERS spectra of adsorbed ATU on a roughened Cu electrode in 11 mM ATU + 1.0 M  $\text{H}_2\text{SO}_4$  solution at different potentials from 0.00 V to  $-0.65$  V

#### 4 Conclusion

The anodic dissolution and electrodeposition of copper and the effect of ATU on the processes in aqueous sulfuric acid have been investigated using CV, EQCM, and SERS. The experimental results demonstrate that the  $M/n$  values for copper dissolution–deposition processes in the solution without ATU are 32.0 and 34.2 g mol<sup>-1</sup>, respectively, indicating that the two-electron transfer reaction is the predominant process. ATU may inhibit copper electrode processes and change the mechanism of the dissolution and deposition of copper. The  $M/n$  values for copper dissolution–deposition processes in the solution with ATU are 61.9 and 65.4 g mol<sup>-1</sup>, respectively, indicating one-electron processes and producing Cu (I) species. Using the SERS technique, we observed the adsorption of ATU at a copper electrode in electrolytes containing ATU in solution. The SERS results demonstrate that ATU adsorbs at the copper surface through its sulfur atom and that the molecular structure of ATU changes significantly after adsorption. The C=C bond in the CH<sub>3</sub>CH=CH– group does not adsorb directly at the copper electrode, but the secondary amino group is nearer to the surface than the primary amino group. Therefore, the whole ATU molecule trends to adsorb in a tilted way through its CH<sub>3</sub>CH=CH– group towards the copper electrode surface. SO<sub>4</sub><sup>2-</sup> and HSO<sub>4</sub><sup>-</sup> can also coadsorb on the protonated –NH (CH<sub>2</sub>CHCH<sub>2</sub>) groups. The results give some insights into these processes.

**Acknowledgment** This work was supported by the Natural Science Foundation of China and the Natural Science Foundation of Fujian Province under Contracts 20433040 and E0310026.

#### References

1. Tantavichet N, Pritzker MD (2005) *Electrochim Acta* 50:1849
2. Cofré P, Bustos A (1994) *J Appl Electrochem* 24:564
3. Yoon S, Schwartz M, Nobe K (1994) *Plat Surf Finish* 81:65
4. Farndon EE, Walsh FC, Campbell SA (1995) *J Appl Electrochem* 25:574
5. Campbell SA, Farndon EE, Walsh FC, Kalaji M (1997) *Trans Inst Met Fin* 75:10
6. Alodan MA, Smyrl WH (1998) *J Electrochem Soc* 145:957
7. Tarallo A, Heerman L (1999) *J Appl Electrochem* 29:585
8. Muresan L, Varvara S, Maurin G, Dorneanu S (2000) *Hydrometallurgy* 54:161
9. Awad MK (2004) *J Electroanal Chem* 567:219
10. Haseeb ASMA, Schilardi PL, Bolzán AB, Piatti RCV, Salvarezza RC, Arvia AJ (2001) *J Electroanal Chem* 500:543
11. Gassa LM, Lambi JN, Bolzán AE, Arvia AJ (2002) *J Electroanal Chem* 527:71
12. Bolzán AE, Wakenge IB, Piatti RCV, Salvarezza RC, Arvia AJ (2001) *J Electroanal Chem* 501:241
13. Łukomska A, Sobkowski J (2006) *J Electroanal Chem* 592:68
14. Bolzán AE, Piatti RCV, Salvarezza RC, Arvia AJ (2002) *J Appl Electrochem* 32:611
15. Alodan MA, Smyrl WH (1998) *Electrochim Acta* 44:299
16. Láng GG, Ujvári M, Horányi G (2002) *J Electroanal Chem* 522:179
17. Loo BH (1982) *Chem Phys Lett* 89:346
18. Brown GM, Hope GA, Schweinsberg DP, Fredericks PM (1995) *J Electroanal Chem* 380:161
19. Brown GM, Hope GA (1995) *J Electroanal Chem* 382:179
20. Brown GM, Hope GA (1996) *J Electroanal Chem* 405:211
21. Brown GM, Hope GA (1996) *J Electroanal Chem* 413:153
22. Zhong QL, Huang QJ, Liu FM, Yao JL, Wang ZQ, Xiong LH, Tian ZQ (1997) *Chin J Appl Chem* 14:13
23. Szymaszek A, Biernat J, Pajdowski L (1997) *Electrochim Acta* 22:359
24. Javet P, Hintermann HE (1969) *Electrochim Acta* 14:527
25. Bertocci U, Turner DR (1997) In: Bard AJ (ed) *Encyclopedia of electrochemistry of the elements*, vol. II. Marcel Dekker, New York
26. Korshin GV, Petukhov AA, Kuznetsov AM, Vyzhimov YM (1991) *Elektrokhimiya* 27:275
27. Mendez S, Andreasen G, Schilardi PL, Figueroa M, Vázquez L, Salvarezza RC, Arvia AJ (1998) *Langmuir* 14:2515
28. Upadhayay DN, Yegnaraman V (2000) *Mat Chem Phys* 62:247
29. Shen CB, Wang SG, Yang HY, Long K, Wang FH (2006) *Appl Surf Sci* 253:2118
30. Dong JH, Song GL, Cao CN, Lin HC (1996) *Acta Phys Chim* 12:252
31. Sauerbrey G (1959) *Z Phys* 155:206
32. Gabrielli C, Keddan M, Tonesi RM (1991) *J Electrochem Soc* 138:2657
33. Tian ZQ, Ren B, DH Wu (2002) *J Phys Chem B* 106:9463
34. Marlot A, Vedel J (1999) *J Electrochem Soc* 146:177
35. Matias JGN, Juliao JF, Soares DM, Gorenstein A (1997) *J Electroanal Chem* 451:163
36. Kemell M, Saloniemi H, Ritala M, Leskelä M (2000) *Electrochim Acta* 45:3737
37. Schumacher R, Borges G, Kanazawa KK (1985) *Surf Sci* 163:L621
38. Liu ZJ, Wu GZ (2004) *Chem Phys Lett* 389:298
39. Swaminathan K, Irving NH (1964) *J Inorg Nucl Chem* 26:1291